Asian Journal of Physics
Vol. 31, Nos 3-6 (2022) 437-448
Available on: www.asianjournalofphysics.com

ap

Random Fiber Lasers: A guided wave optical device for multidisciplinary photonic applications

Anderson S L Gomes

Department of Physics, *Universidade Federal of Pernambuco,*
Cidade Universitária, Recife, PE, 50670-901, Brazil

Dedicated to Professor Bishnu P Pal for his enormous contributions to the advancement of research and education in science and technology through his unique vision and outstanding dedication

This paper presents a review of the *state-of-the-art* in random fiber lasers (RFL), which are guided wave optical devices similar to fiber lasers but with an important difference: RFL relies on scattering to provide the optical feedback mechanism required for laser action in a gain medium, whereas in the conventional laser or fiber laser this is provided by two static mirrors. After introducing the basics of RFLs and highlighting the main developments since 2007, some applications will be described in the fields of optical imaging, Lévy-like behavior, turbulence and photonic spin-glass.

Keywords: Fiber Lasers, Random Fiber Lasers, Photonic Devices, Diagnostic by Imaging, Complex Systems.

1 Introduction

A laser source [1] is certainly the most widely used optical device developed to date, due to its multidisciplinary applicability and its endless scientific developments, which arise from its optical characteristics: the photons generated by a laser source are emitted in a single direction, are temporally coherent and are monochromatic, whose emission wavelength is uniquely determined by a combination of the so-called laser medium – or gain medium – and the laser cavity, generally composed of two parallel mirrors. To assemble a laser source, besides the gain medium and the laser cavity, a pump source is necessary. The mechanisms behind the laser emission relies on light absorption, stimulated emission, population inversion, gain and oscillation [1]. Stimulated emission is a process proposed first by Einstein in 1905 [2], without ever thinking of an optical source. It was only in 1958 that such mechanism was exploited to provide gain and oscillation in the microwave region, giving rise to the MASER [3]. It was soon realized that it could also operate in the visible spectral region, and, therefore, the LASER was demonstrated by T Maiman in 1960 [4]. This well-known history opened the scientific and technological exploitation of operating lasers in configurations as continuous wave, pulsed (Q-switched, mode-locked, and so on), besides a fantastic number of laser sources covering from the deep UV to the far infrared, from highly stable and narrow spectral lines to ultrabroadband operation and even supercontinuum spectral operation besides generating attosecond pulses, most of these sources are now commercially available. Such development led to several Nobel prizes to researchers who contributed to the laser field, and an excellent updated review with a timeline for Nobel prizes related to lasers can be found in ref [5].

While lasers were being developed, optical fibers with acceptable optical losses were already being developed in the early 1960's [6], whilst simultaneously specialty fibers, such as those doped with rare earth

Corresponding author
e mail: andersonslgomes@gmail.com (Anderson S L Gomes)

ions were developed and used to demonstrate the fiber lasers and amplifiers [7,8]. In this guided geometry, the light emission is optically confined and guided along the fiber core, and by placing the gain fiber between two mirrors, or by suitable coatings on the fiber ends, a fiber laser as the one-dimensional version of the laser has been demonstrated. Nowadays, a fiber laser is a very compact device whereby the mirrors or coating on the fiber ends are replaced by fiber Bragg gratings (FBGs) [9] which are directly inscribed in the fiber core, and the fiber laser is directly pumped by semiconductor lasers. Besides using rare earth doped materials such neodymium, erbium or thulium, the inherent Raman or Brillouin processes in optical fibers have been used to develop the so-called Raman fiber lasers [10] or Brillouin fiber lasers [11].

In this article - dedicated to of Professor Bishnu Pal, who has tremendously contributed to the field of optical guided waves - I would like to bring to the reader's attention an important variation of the "classical" laser as described above (which employs two conventional mirrors to provide optical feedback) to the so-called random lasers, a class of laser devices which keeps all the ingredients of a conventional laser but whose optical feedback is provided by scattering of light in a randomly disordered medium. Such a system was first proposed by V S Letokhov in 1967 [12], and a very thorough and updated review on the subject can be found in ref [13]. The first unambiguous experimental demonstration of a random laser was published in 1994 [14], where the authors employed Rhodamine B as the gain medium and TiO_2 nanoparticles (250nm diameter) as the scattering medium, and this colloid, when pumped by the second harmonic of a pulsed (10Hz, 10ns) Nd:YAG laser, generated coherent emission around 600nm. The history and spectacular development of random lasers in 2D (planar geometry) or 3D (bulk) architectures between 1994 and June 2021 can be found in ref [13] and other earlier reviews therein. In this article, I concentrate on random fiber lasers (RFLs), first demonstrated in 2007 [15] by our group in Brazil, which opened avenues for a wide range of publications covering different designs and architectures for RFL, and their applications.

To understand the fundamentals of guided wave optics, required to understand and appreciate fiber lasers and random fiber lasers, the readers are referred to the books by Bishnu Pal [16] and G P Agrawal [17] which are authoritative documents, and lay down the fundamentals of light propagation in fibers.

In the remaining sections of this article, I shall describe in a summarized manner in section 2 the basics of RFL and their developments since 2007. In section 3, I shall highlight some chosen (a personal choice) applications, including its use as optical sources for imaging, sensors, optical amplifiers and as a photonic platform for studies of Lévy-like and turbulence-like behavior of light, and replica symmetry breaking, a feature originally studied in magnetism, and which led to the recent Nobel prize nomination (one of the three winners) to Giorgio Parisi, which arises from a phase transition from paramagnetic to spin glass phase. I will describe the photonic process analogous to such a phase transition. I shall conclude in section 4 with a brief outlook on the field.

2 Random Fiber Lasers (RFL)

As mentioned before, a fiber laser is nowadays a very simple device consisting of a gain fiber with inscribed FBGs (Fiber Bragg Gratings) reflecting at the desired wavelength when properly pumped. It can be a very compact device, and therefore finds a great number of applications. It can also operate at high power and in the femtosecond regime [18]. RFLs were first demonstrated using a colloid similar to that used in ref [14], as the gain medium. This consisted of Rhodamine B and TiO_2 nanoparticles, placed in the hollow core of a microstructured fiber, as first reported in 2007 [15]. Since then, a spectacular growth has occurred, particularly triggered by the work of Kashyap's group [19] and Turitsyn's group [20]. Figure 1 pictorially depicts the kind of RFLs already developed by several research groups worldwide, and the reader is referred to [13] and references therein for a deeper dive into the subject.

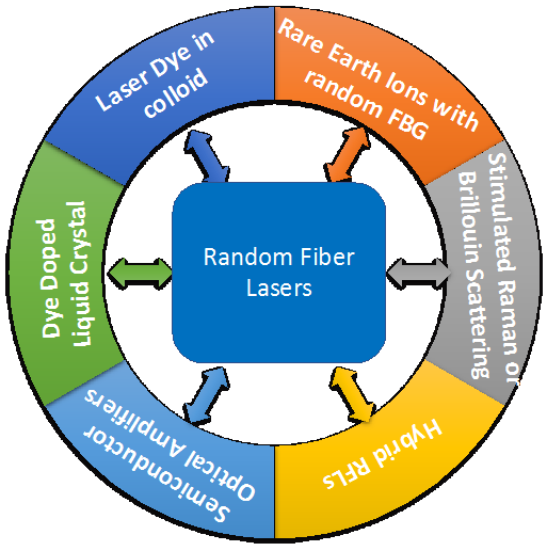

Fig 1. Pictorial view of the kinds of RFLs developed since 2007. Starting from using a colloidal solution of laser dye and nanoparticles, then rare earth doped fiber (Erbium) with random FBG was followed using conventional fibers exploiting Raman and/or Brillouin as the gain media and Rayleigh scattering as the scattering media. In the subsequent years, hybrid schemes using a combination of the former were introduced, then the use of semiconductor optical amplifiers and even dye doped liquid crystals. Hybrid RFLs have already combined most of these RFLs as reported in ref [13].

To exemplify two types of RFLs, we summarize the results of a Raman RFL operating at 1550nm [21] and a hybrid electronically addressable RFL (HEAR laser), which exploits a combination of SOA (Semiconductor optical Amplifier) and Erbium doped fiber (EDF) [22].

2.1 A Random RFL

Figure 2 shows the experimental setup and Raman RFL laser characterization. The system was used to characterize intensity statistics of the spectral components, which is not going to be dealt with in this section. The full details can be found in ref [21], but in short, the setup includes two parts: the Raman RFL system itself and the intensity of the spectral component, as measured in the experiment. A commercial Raman laser with 1455 nm of center wavelength was used as the pump source for the Raman RFL and is injected into a 5 km SMF from the common port of WDM1 (Wavelength Division Multiplexer). The other end of the 5 km SMF (Single Mode Fiber) provides the output for the random lasing emission. As can be seen in the figure, a highly reflective FBG with 1550 nm center wavelength connects to the 1550 nm port of WDM1, forming a half-open cavity structure by combining the random distributed Rayleigh scattering in the SMF. The 5km SMF is angle cleaved to avoid reflection. The gain for the 1550 nm random lasing emission is provided with the distributed Raman gain in the 5km fiber. Raman RFLs is one of the most exploited RFLs, with high power and cascaded emission widely demonstrated, as reviewed in [13].

2.2 A hybrid electronically addressable RFL (*HEAR Laser*)

As the second example reported in ref [22], a novel hybrid scheme using a SOA and an 81m long EDF were combined to implement a hybrid electronically addressable RFL. The scheme is shown in Fig 3(A) and can potentially work at repetition rate of several MHz controlled in the SOA, which can electronically address the operation point along the EDF fiber length with ~1m spatial resolution, which defines where the

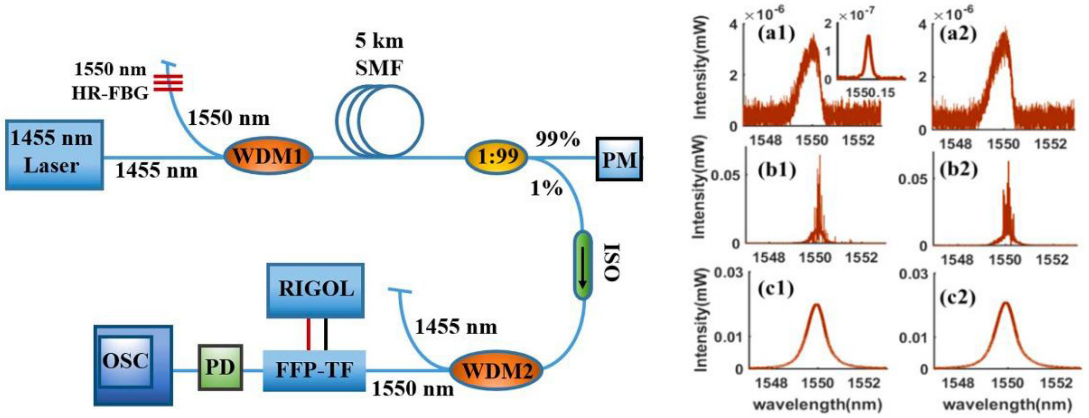

(A) (B)

Fig 2. (A) Experimental setup for measuring the intensity of spectral component of the Raman RFL system. WDM, wavelength division multiplexer; SMF, single-mode fiber; HR-FBG, highly reflective fiber Bragg grating; OC, optical coupler; PM, power meter; ISO, isolator; FFP-TF, fiber Fabry–Perot tunable filter; PD, photodetector; OSC, oscilloscope; (B) Representative spectra obtained (a1) and (a2) below threshold (Pp/Pth 0.9), (b1) and (b2) around threshold (Pp/Pth 1.1), and (c1) and (c2) above threshold (Pp/Pth 1.3). The inset of (a1) presents the filtered spectral component for Pp/Pth 0.9. From ref [21], with permission.

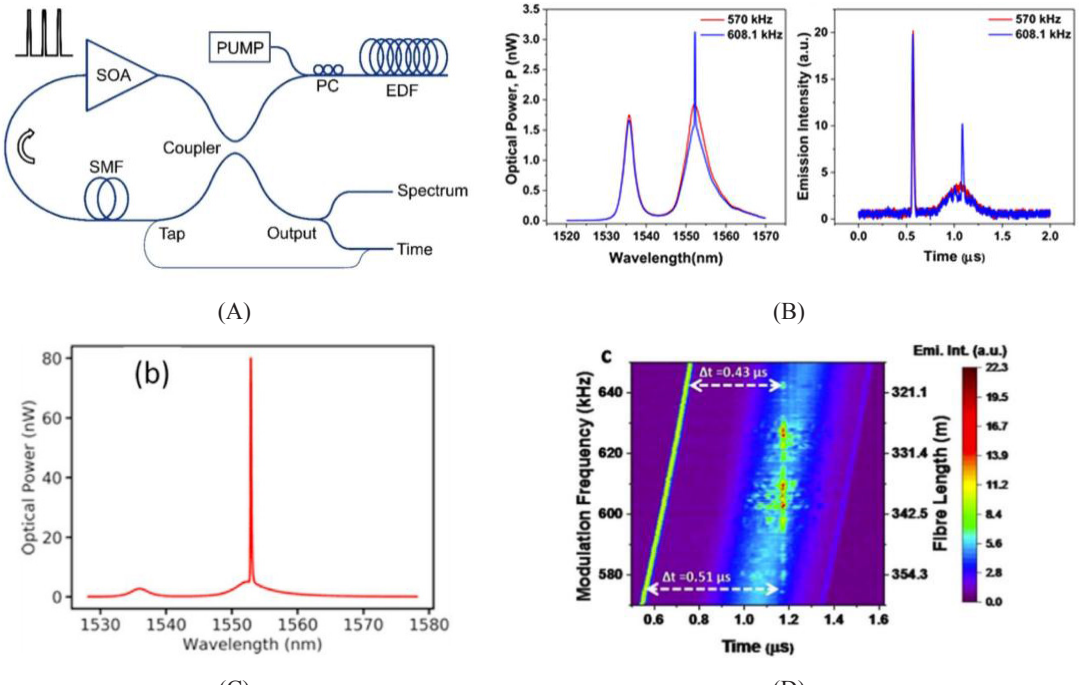

(A) (B)

(C) (D)

Fig 3. (a) Simplified schematic diagram for the HEAR laser. Gain is provided by the pulsed unidirectional SOA and by the cw pumped Er^{3+} doped fiber. (b) Spectral emission of HEAR laser, showing the dual Er^{3+} band, with narrow laser emission in the second band. (c) Optimized HEAR laser emission. (d) Contour plot of temporal response, see Ref [22] for details (a, c and d adapted from Ref [22], with permission).

effective feedback scattering takes place. To warrant population inversion in the CW regime, the EDF was optically biased, while the SOA operated in a pulsed mode (up to hundreds of kHz), thus operating as a fast modulator with gain. The EDF was pumped at 1480 nm, while the SOA composed of a loop mirror electrically excited by 16 ns pulses at frequencies around 600 kHz. Random laser oscillation was obtained by synchronizing the frequency of the modulated SOA with the back reflection to the SOA of backscattered light from a given section of the EDF. This innovative synchronous process provided the required scattering feedback mechanism characteristic of RLs and allowed the electronically tunability to different positions along the EDF. Figure 3(B) left shows the spectrum above threshold. The two erbium bands originated from ASE are seen, as well as the laser emission (narrow line) at 1552 nm. Simultaneously, the temporal behavior above threshold was detected and shown in Fig 3(B) right. It shows the SOA pulse (red/blue), the ASE pulse (red), and the lasing pulse (blue peak) when synchronization is introduced. Figure 3(C) shows an optimized spectrum output. The contour plot of the timing of the laser pulses is shown in Fig 3(D), obtained by varying the modulation frequency. The data was built by fixing the RL pulses at the tap port as a vertical line at a certain time (1.18 μs), the effect of varying the frequency of the drive pulses could be observed. To address different segments of the EDF, one can simply adjust the modulation frequency. Sensing applications for the hybrid RFL can certainly be envisaged.

3 Random fiber laser applications

Applications of RFLs already cover a diversity of fields, including biophotonics, sensing, optical amplification and more recently complex systems and statistical physics. Besides the review in ref [13], the readers specially interested in RFLs and applications, particularly optical amplification and sensing should also look at refs [23-26]. For a review of applications in Lévy statistics and glassy behavior of light, please see ref [27]. I have chosen two examples: the use of a RFL for high contrast speckle-free dental bio-imaging [28] and its use as a photonic platform for simultaneous studies of turbulence and glassy behavior of light [29]. The last referenced article, as we will point out in more detail, has been cited as the connection between the work of two of the three Nobel prize winners of 2021, Hasselman and Parisi, as nominally described in the report of the Nobel Committee for Physics 2021 [30].

3.1 RFL as a speckle-free optical source for dental bio-imaging

The experimental setup for the imaging experiment is reproduced in Fig 4(A). The RFL source is constructed using a half-opened structure composed of a fiber loop mirror (from a 3dB coupler, see figure) and 25 km-length single mode fiber (SMF). A Raman pump source (1455 nm) is injected into the SMF through a 1455/1550 nm wavelength division multiplexer (WDM 1). As can be seen in the figure, WDM2 is used at the end of the SMF in order to split out the residual pump light and make sure only the generated RFL injects into the imaging part. An isolator (ISO) eliminates light reflection, assuring that the laser feedback is provided only by the randomly distributed Rayleigh scattering. A variable optical attenuator (VOA) is used for power adjustment at the input of the imaging system. For comparison of the imaging results, two typical sources are employed: an ASE light source, based on an EDF and a narrow line width laser (NLL 1550nm). The optical spectra of the three sources are shown in Fig 4(B). The full width at half maxima (FWHM) of the RFL is ~1.5 nm (at the pump power of 33.4 dBm). The FWHM of ASE is 4.7 times broader than the RFL and the NLL has the narrowest FWHM, ~0.01 nm. The calculated coherence length, $\Delta c = \lambda^2/\Delta\lambda$, where λ and $\Delta\lambda$ are the center wavelength and spectral bandwidth respectively, shows that the RFL has a shorter coherence length than the NLL. The imaging part of the experiment (to the left after the VOA, Variable Optical Attenuator) employs, as in ref [31], a backscattering configuration. An extra-large mode area step-index MMF (Multimode Fiber) was spliced after the VOA and before the imaging system to further reduce the spatial coherence of light source(s). The illumination light from the MMF is properly collimated (see details in ref 28). The reflected light from the sample is directed to the CCD (Charge Coupled Device) via the beam-splitter. Each tooth sample was sectioned mesiodistally in parallel along the axis of the crown.

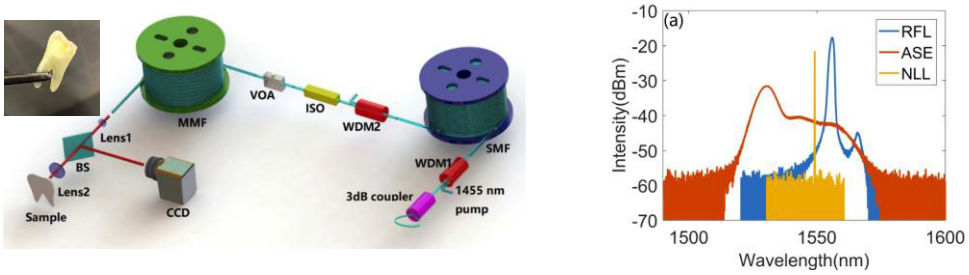

(A) (B)

Fig 4. (A) Schematic of experimental setup. WDM, wavelength division multiplexer. SMF, single mode fiber. ISO, isolator. VOA, variable optical attenuator. MMF, multimode fiber. BS, beam splitter; (B) spectrum of RFL, ASE, and NLL. The inset picture, left in Fig (A), shows the tooth sample.

The imaging result for all three optical sources employed can be seen in Fig 5(A), left to right, tooth imaging using as optical sources RFL, ASE and NLL, respectively. The enamel is a high transmittance medium (compared to other parts of the tooth), therefore most of the light penetrates and only a small percentage is scattered back to the detector. As a result, the enamel (which is a ~1mm layer covering the dentin) part appears as dark region, while the dentin has high backscattering and appears as a bright region. Moreover, the mineral loss of a carious region in enamel would cause more than two orders of magnitude increase in scattering coefficient and as a consequence appears as a bright region in backscattering image. This difference in scattering coefficient means healthy enamel and carious tissues have a high difference in contrast and can be easily detected. As pointed out in [28], for RFL and ASE (Amplified Spontaneous Emission), the enamel, dentin, and demineralized enamel regions of tooth specimen can be clearly identified, while for NLL (Narrow Linewidth Laser), strong speckle patterns occur and blur the image, as seen in Fig 5(A). Furthermore, in Fig 5(B), a comparison of RFL generated imaging with two different imaging methods, i.e., radiography and microscope, is shown. Of course, microscopy is not clinically used, whereas radiography is the clinical standard. In part (b, center) the radiography could only identify enamel and dentin but is not capable to properly detect details in these regions. Conversely, in part (a, left) of Fig 5(B) the RFL based backscattering image method could further distinguish the mineral concentration showing different brightness in the dentin region. This is due to the penetration depth provided by the NIR wavelength employed. Finally, regarding part (c, right) in the figure, employing an optical microscope, one can see the crack in the enamel, but the dentin region appears uniform.

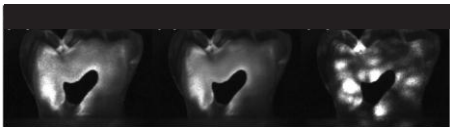

(A)

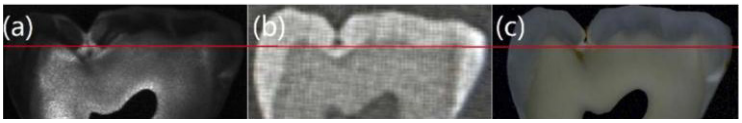

(B)

Fig 5. (A) left to right, tooth imaging result using as optical sources RFL, ASE and NLL, respectively. (B) Imaging from different methods. (a) RFL, (b) Radiography, (c) Microscope. Red line shown was employed for intensity scale measurements (see ref 28 for details. Figure 5 is adapted from ref [28], with permission).

To conclude this section, we just point out that, since the pioneering work of Redding and co-workers [32], who first demonstrated the use of random lasers as speckle-free sources for optical bio-imaging, this application has been provided the most applications so far for RL and RFLs. The work summarized here shows this is a good assumption.

3.2 RFL as photonic platform for simultaneous studies of turbulence and glassy behavior of light

The 2021 Nobel Prize in Physics was awarded to Syukuro Manabe, Klaus Hasselmann and Giorgio Parisi "for groundbreaking contributions to our understanding of complex systems" [30]. Among the phenomena classified within the realm of complex systems, turbulence [33], a subject found in many natural and artificial environments, and spin glass behavior [34], first studied in magnetic materials, have been the subject of intense research for many decades. Whilst turbulence has already been studied in the optical regime, including fiber lasers [35] and random fiber lasers [36] among others, spin glass behavior was only experimentally demonstrated in a photonic system in 2015 [37], when the first ever experimental demonstration of the replica symmetry breaking (RSB) theory in any physical system was published, using a random laser to describe the photonic analog of the proposed RSB theory by Giorgio Parisi in 1979 (see [34] and refs therein). It is the work of Parisi on RSB and spin glasses who led the Nobel prize committee to award him "for the discovery of the interplay of disorder and fluctuations in physical systems from atomic to planetary scales."

Shortly after the work of Ghofraniha and co-workers in 2015 demonstrating RSB in random lasers, our group has expanded this photonic analogy to several other random lasers and random fiber laser systems, as reviewed in refs [13,27].

The example chosen to be reviewed here reports the first evidence of the coexistence of two of the most challenging phenomena in complex systems: turbulence and spin glasses. The photonics platform for such demonstration was a RFL, which displays all essential ingredients required to observe both behaviours, namely disorder, frustration, nonlinearity, turbulent energy cascades and intermittent energy flux between fluctuation scales. The results were obtained from a single set of measurements, whose details are described in ref [29]. Such results solved a long-standing open question raised more than 20 years ago by the authors of ref [33]: would there be an intrinsic connection between turbulence and spin glass? The first evidence of such connection appeared when approaching turbulence and interface dynamics through the Burgers equation (see ref 33).

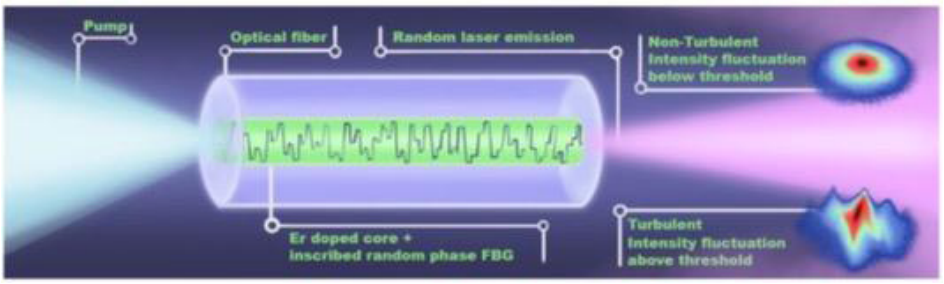

Fig 6. The photonic random fiber laser system. Pictorial description of the 30 cm long erbium-doped RFL with a large number (~103) of specially-designed random fiber Bragg gratings inscribed in the core. The pump source was a semiconductor laser operating in the CW regime at 1480.0 nm. The multimode RFL emission peaks at 1540.0 nm. A rather extensive number of 150,000 spectra were collected at the excitation power above the RFL threshold, P/Pth = 2.92. Below the threshold, a replica-symmetric prelasing phase sets in with non-turbulent behavior. In contrast, at P/Pth = 2.92 the RFL system exhibits the coexistence of photonic RSB spin glass and turbulence-like behaviors in the distribution of intensity increments between successive spectra. From ref [29], with permission).

The experiment was performed using the same RFL as first reported by Gagné and Kashyap [19], which our group employed extensively in a diversity of applications [29,36,38,39,40]. The RFL details are given in the caption of Fig 6, with a pictorial view of the device.

The experimental data obtained consisted of a set of spectra (150,000) for excitation powers below and above threshold. These spectra were independently analyzed using the appropriate equations for either turbulence-like behavior [36] or glassy behavior [40]. The equations governing either behavior "do not talk to each other", and we are not reproducing them here, interested readers should refer to the cited references. The key factors are that for the RSB, a Parisi parameter is defined, whereas for turbulence, an incremental quantity is relevant. Of interest to the coexistence of the turbulence and spin glass behavior is the key equation of ref [29], reproduced below, where a so-called photonic Pearson correlation *coefficient*, Q, was introduced:

$$Q_{\alpha\beta,\tau} = \frac{\sum_k \delta_{\alpha\tau}(k)\,\delta_{\beta\tau}(k)}{\sqrt{\sum_k \delta^2_{\alpha t}(k)}\,\sqrt{\sum_k \delta^2_{\beta t}(k)}} \tag{1}$$

In fact, for $\tau = 0$ (a time scale) it recovers the Parisi overlap parameter of the photonic glassy phase, $Q_{\alpha\beta,\tau} = 0 = q\alpha\beta$. On the other hand, for $\tau \geq 1$ the Pearson coefficient infers the turbulence phenomenon. As demonstrated in [29], the intermittency, which is the maximum turbulence-like signature, manifests itself at the shortest time scale $\tau = 1$. By contrast, for $\tau >> 1$ the short-time-scale effects and intermittency rapidly fade away and a crossover takes place to the non-turbulent (Gaussian) behavior. The experimental results are shown in Figs 7 and 8. In Fig 7, the RFL characterization shows (a) the emission bandwidth below and above threshold and (b) the linewidth narrowing and emitted intensity as a function of pump power (normalized to the threshold power).

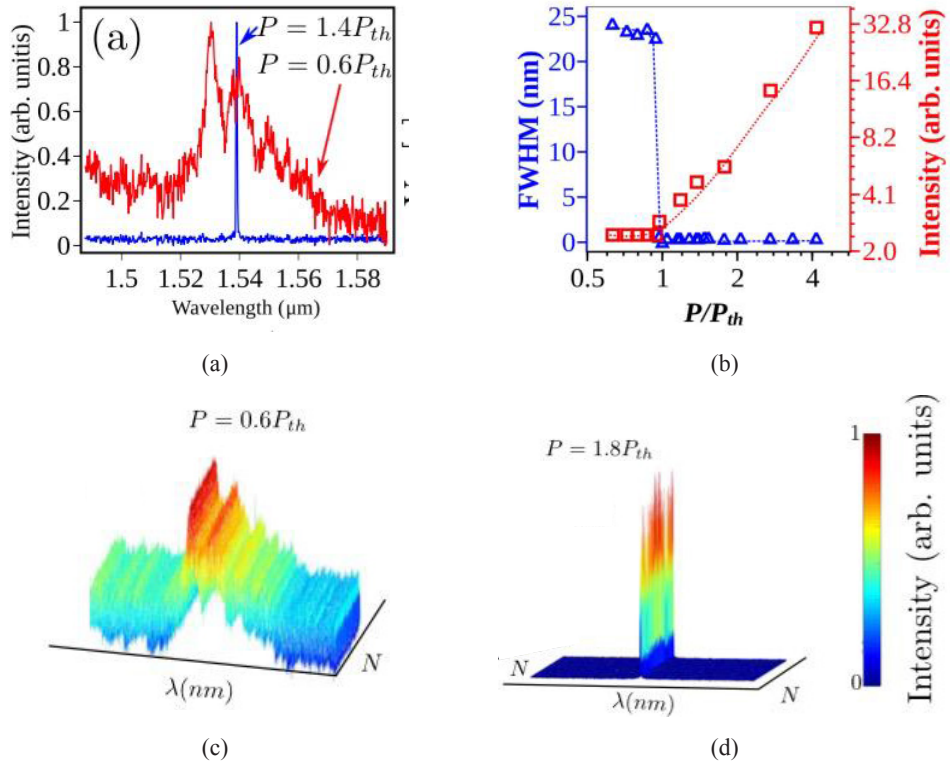

(a) (b)

(c) (d)

Fig 7. Experimental characterization of the RFL used in the turbulence and spin glasses experiment (adapted from ref [38]).

Figures 7(c) and (d) show a set of spectra below and above threshold, illustrating the kind of measurement obtained for which the equations are applied to fit the data. As already mentioned, 150,000 spectra were collected at the excitation power above the RFL threshold, P/Pth = 2.92 for this experiment.

The results of the analysis of such type of data using Eq (1) are shown in Fig 8. It suffices, in this review, to say that the points are the experimental data, and the lines are the theoretical fits in the two regimes that can be assessed using the photonics Pearson correlation function of Eq (1), whose details can be seen in ref [29]. The top part of the figure reveals the turbulent regime, for which the temporal parameter $\tau = 1$, and the y-scale represents increments. On the other hand, the bottom figure for $\tau >> 1$, therefore in the non-turbulent regime, indeed reproduce the bimodal characteristics of replica symmetry breaking in the spin glass regime.

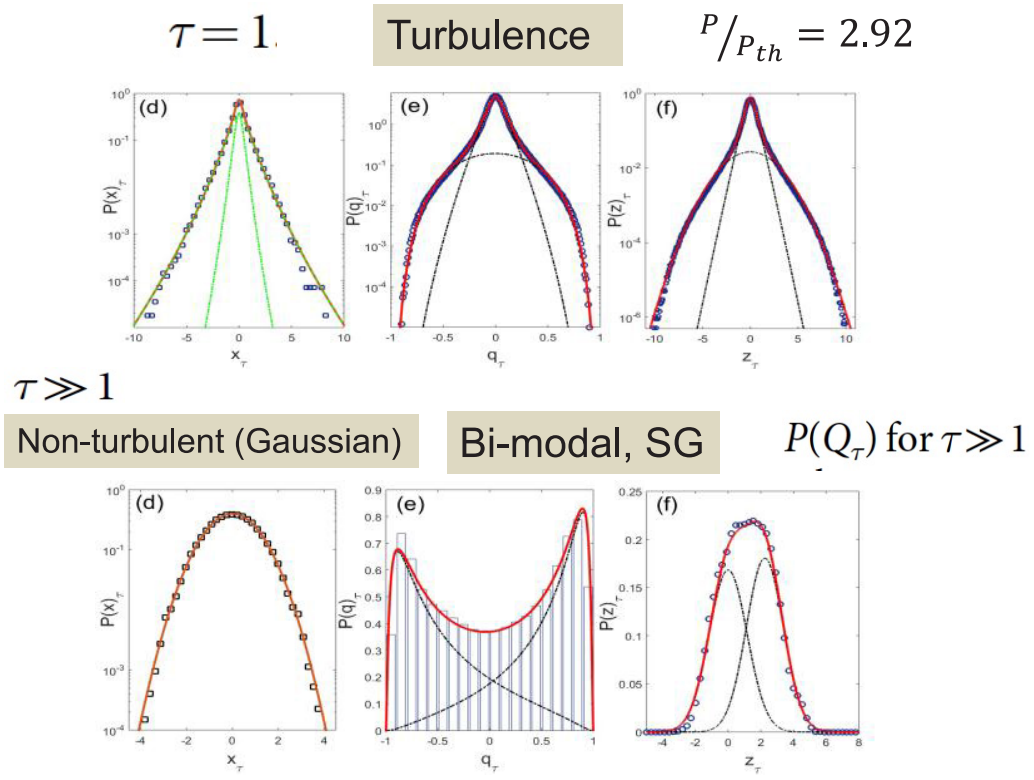

Fig 8. Theoretical fits from Eq (1) applied to the same set of experimental data, showing both turbulent and glassy photonic regimes in the RFL. Adapted from ref [29], with permission.

Besides the demonstration of the coexistence of turbulence and spin-glass behavior in a photonic system, our work reported in ref [29] goes even further. In page 11 of ref [30], where the Nobel committee describes the scientific ground for nominating the winners of the Nobel prize, they nominally highlight our work of ref [29], as follows: "Importantly, experimental evidence of replica symmetry breaking has been provided in systems using random lasers [30,33,99,108], in plane cavity lasers without disorder but with frustration between interacting lasing modes without added disorder [7,74], and in nonlinear optical propagation through photorefractive disordered waveguides [90]. Finally, the nature of the random laser system allows for the concomitant observation of replica symmetry breaking and connection between spin-glasses and turbulence [34], particularly nonlinear wave interactions, which link the early work of Hasselmann [40,41] to that of Parisi and to the role of disorder and fluctuations in complex systems in general".

It is, therefore, very clear the importance of random lasers and random fiber lasers in nowadays multidisciplinary world, where scientists from different fields can get together to advance science, whose final results should impact society.

4 Conclusion and outlook

As an overall conclusion, random lasers and random fiber lasers are guided wave optical devices highly likely to find a significant number of multidisciplinary photonic applications. We have given a few examples of their importance in biophotonics and complex systems. It is a very modern device, with modern applications. Looking forward to new developments, from the technological point of view electrically pumped RLs should be further developed [41] and both, RLs and RFLs should be more exploited in applications as sensing devices or optical sources, for instance, in environment or nanobiotechnology challenges. From more scientific point of view, further developments of quantum behavior of RL and RFLs, for instance studying Floquet systems [39], where quantum behavior can be manifested, is one way to pursue further applications of RFL.

NOTE FROM THE AUTHOR: The text in italic was directly reproduced from ref 30, which is freely available on the Nobel Committee website. Ref 34 is our ref 29).

Acknowledgements

The research described in this publication was made possible due to the continuous financial support from the Brazilian Agencies CNPq, CAPES and FACEPE. Even more important was the involvement and decisive contribution of several M Sc and Ph D students, post-docs and scientific collaborators worldwide, from Brazil, China and Canada, whose collaborative work has been cited in this review paper.

References

1. Siegman A E, Lasers, University Science Books, (Mill Valley, CA), 1986.
2. Einstein A, On the Quantum Theory of Radiation, *Phys Zs*, 18(1917)121.
3. Schawlow A L, Townes C H, Infrared and Optical Masers, *Phys Rev*, 112(1958)1940; doi.org/10.1103/PhysRev.112.1940.
4. Maiman T, Stimulated Optical Radiation in Ruby, *Nature*, 187(1960)493–494.
5. Dudley J, Light, Lasers, and the Nobel Prize, *Adv Photon*, 2(2020)050501; doi.org/10.1117/1.AP.2.5.050501.
6. https://www.nobelprize.org/prizes/physics/2009/kao/facts/
7. Snitzer E, Optical maser action of Nd^{+3} in barium crown glass, *Phys Rev Lett*, 7(1961)444–446.
8. Poole S B, Payne D N, Fermann M E, Fabrication of low-loss optical fibres containing rare-earth ions, *Electron Lett*, 21(1985)737–738.
9. Kashyap R, Fiber Bragg Gratings, 2nd Edn, (Academic Press), 2009.
10. Feng Y (Ed), Raman Fiber Lasers, (Springer), 2017.
11. Dong L, Samson B, Fiber Lasers: Basics, Technology, and Applications, (Taylor and Francis Group), 2016.
12. Letokhov V S, Stimulated emission of an ensemble of scattering particles with negative absorption, *JETP Lett* (Engl Transl), 5(1967)212–215.
13. Gomes A S L, Moura A L, de Araújo C B, Raposo E P, Recent advances and applications of random lasers and random fiber lasers, *Prog Quantum. Electron*,78(2021)100343; doi.org/10.1016/j.pquantelec.2021.100343.
14. Lawandy N M, Balachandran R M, Gomes A S L, Sauvain E, Laser action in strongly scattering media, *Nature* 368(1994)436–438.
15. de Matos C J S, Menezes L D S, Brito-Silva A M, Gamez M A M, Gomes A S L, de Araújo C B, Random fiber laser, *Phys Rev Lett*, 99(2007)153903; doi.org/10.1088/1612-202X/ac3247.

16. Pal B (ed), Guided Wave Optical Components and Devices: Basics, Technology, and Applications, (Elsevier), 2006.
17. Agrawal G P, Nonlinear Fiber Optics, 5th Edn, (Academic Press), 2013.
18. Zhang M, Kelleher E J R, Popov S V, Taylor J R, Ultrafast fibre laser sources: Examples of recent developments, *Opt Fiber Technol*, 20(2014)666-677.
19. Gagne M, Kashyap R, Demonstration of a 3 mW threshold Er-doped random fiber laser based on a unique fiber Bragg grating, *Opt Express*, 17(2009)19067–19074.
20. Turitsyn S K, Babin S A, El-Taher A E, Harper P, Churkin D V, Kablukov S I, Ania-Castanon J D, Karalekas V, Podivilov E V, Random distributed feedback fibre laser, *Nat Photonics*, 4(2010)231–235.
21. Li J, Wu H, Wang Z, Lin S, Lu C, Raposo E P, Gomes A S L, Rao Y, Lévy spectral intensity statistics in a Raman random fiber laser, *Opt Lett*, 44(2019)2799–2802.
22. Margulis W, Das A, von der Weid J P, Gomes A S L, Hybrid electronically addressable random fiber laser, *Opt Express*, 28(2020)23338–3396.
23. Rao Y J, Zhang W L, Recent progress in random fiber lasers, 2013 12th International Conference on Optical Communications and Networks 1-4, (2013) ICOCN, doi: 10.1109/ICOCN.2013.6617202.
24. Turitsyn S K, Babin S A, Churkin D V, Vatnik I D, Nikulin M, Podivilov E V, Random distributed feedback fibre lasers, *Phys Rep*, 542(2014)133–193.
25. Churkin D V, Sugavanam S, Vatnik I D, Wang Z, Podivilov E V, Babin S A, Rao Y, Turitsyn S K, Recent advances in fundamentals and applications of random fiber lasers, *Adv Opt Photon*, 7(2015)516–569.
26. Chen H, Gao S, Zhang M, Zhang J, Qiao L, Wang T, Gao F, Hu X, Li S, Zhu Y, Advances in Random Fiber Lasers and Their Sensing Application, *Sensors*, 20(2020)6122–6141.
27. de Araújo C B, Gomes A S L, Raposo E P, Levy Statistics and the Glassy Behavior of Light in Random Fiber Lasers, *Appl Sci*, 7(2017)644–662.
28. Guo J Y, Zhang W L, Rao Y J, Zhang H H, Ma R, Lins I C X, Lopes D S, Gomes A S L, High contrast speckle-free dental bio-imaging using random fiber laser in backscattering configuration, *OSA Continuum*, 3 (2020)759–767.
29. Gonzalez I R R, Raposo E P, Macedo A M S, Menezes L S, A S L Gomes, Coexistence of turbulence-like and glassy behavior in a photonic system, *Sci Rep*, 8(2018)17046; doi.org/10.1038/s41598-018-35434-z.
30. Report of the Nobel Committee for Physics, Scientific Background on the Nobel Prize in Physics 2021. https://www.nobelprize.org/prizes/physics/2021/advanced-information/
31. Carvalho M T, Lotay A S, Kenny F M, Girkin J M, Gomes A S L, Random laser illumination: an ideal source for biomedical polarization imaging? in Multimodal Biomedical Imaging, XI(2016)9701; doi.org/10.1117/12.2209623.
32. Redding B, Choma M A and Cao H, Speckle-free laser imaging using random laser illumination, *Nat Photonics*, 6(2012)355–359.
33. Bohr T, Jensen M H, Paladin G, Vulpiani A, Dynamical Systems Approach to Turbulence, (Cambridge University Press, Cambridge),1998.
34. Mézard M, Parisi G, Virasoro M A, Spin Glass Theory and Beyond, (World Scientific, Singapore), 1987.
35. Turitsyna E G, Smirnov S V, Sugavanam S, Tarasov N, Shu X, Babin S A, Podivilov E V, Churkin D V, Falkovich G, Turitsyn S K, The laminar-turbulent transition in a fibre laser, *Nat Photon*, 7(2013)783–786.
36. González I R, Lima B C, Pincheira P I R, Brum A A, Macêdo A M S, Vasconcelos G L, Menezes L S, Raposo E P, Gomes A S L, Kashyap R, Turbulence hierarchy in a random fibre laser, *Nat Commun*, 8(2017)15731; doi.org/10.1038/ncomms15731.
37. Ghofraniha N, Viola I, Maria F D, Barbarella G, Gigli G, Leuzzi L, Conti C, Experimental evidence of replica symmetry breaking in random lasers, *Nat Commun*, 6(2015)6058; doi.org/10.1038/ncomms7058
38. Lima B C, Gomes A S L, Pincheira P I R, Moura A L, Gagné M, Raposo E P, de Araújo, C B, Kashyap R, Observation of Lévy statistics in one-dimensional erbium-based random fiber laser, *J Opt Soc Am B*, 34(2017)293–299.

39. Raposo E P, González I R R, Macêdo A M S, Lima B C, Kashyap R, Menezes L S, Gomes A S L, Evidence of Floquet phase in a photonic system, *Phys Rev Lett*, 122(2019)143903; doi.org/10.1103/PhysRevLett.122.143903.

40. Gomes A S L, Lima B C, Pincheira P I R, Moura A L, Gagné M, Raposo E P, de Araújo C B, Kashyap R, Glassy behavior in a one-dimensional continuous-wave erbium-doped random fiber laser, *Phys Rev A*, 94(2016)011801(R); doi.org/10.1103/PhysRevA.94.011801.

41. Yu S F, Electrically pumped random lasers, J Phys D: Appl Phys, 48 (2015) 483,001; doi.org/10.1088/0022-3727/48/48/483001.

[*Received*: 12.01.2022; *revised recd*: 12.03.2022; *accepted*: 20.03.2022]

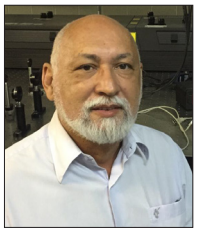

Anderson Stevens Leônidas Gomes was born in Recife, Pernambuco. He completed his graduation (1978) and master's (1982) in Physics from the Physics Department of the Universidade Federal of Pernambuco (UFPE). His doctorate in Laser Physics was obtained at the Imperial College of Science, Technology and Medicine (1986), and postdoctoral at Brown University USA (1992). He is presently a Professor of Physics at the Physics Department of UFPE. His scientific activities are in the areas of laser applications in nano and biophotonics, non-linear optics and non-linear photonic devices, where he has co-authored more than 300 scientific publications, H-index Google Scholar: 48; H-index Web of Science: 36. He has supervised 39 master's dissertations and 20 doctoral theses. He holds a CNPq Fellowship level 1A (highest level). He is a Fellow of OPTICA (former OSA), where he was President of the International Council (2011-2012). He is also a member of the Brazilian Physics Society (SBF), SPIE and the Brazilian Academy for the Progress of Sciences (SBPC). He was Associate Editor of Advances in Optics and Photonics (OPTICA Publishers) and is currently Associate Editor of Light: Science and Applications, Nature Group.

He has served on several Brazilian science policy committees for higher education, coordinated the area of Physics and Astronomy at CAPES (Brazilian Agency of Education, 2008-2010), and is a former member of the Physics Council of CNPq (Brazilian Science Agency). In 2010, he was awarded and admitted to the National Order of Scientific Merit, Commander Class in the area of Physical Sciences (Decree of December 27, 2010) and is a Full Member of the Brazilian Academy of Sciences and a Regional Vice-President for the Northeast of Brazil. He is currently a member of the Council of the Brazilian Physics Society (SBF) and Brazilian Society for Advancement of Science (SBPC) .

In 2010 he was Secretary of State for Science, Technology and Environment of Pernambuco (April to December 2010), and was Secretary of State for Education of Pernambuco, from January 2011 to December 2012.

On the national level, He is a member of the Council of the National Brazilian Fund for Development of Science and Technology, a Federal Government committee responsible for the budget from the national fund to S&T Brazilian institutions and sectorial funds, and also of the Photonics Consultive Committee of the Ministry of Science, Technology and Innovation.